J. Fluid Mech. (1982), *vol.* 116, *pp.* 379–391
Printed in Great Britain

Dynamics of an impinging jet. Part 2. The noise generation

By NAGY S. NOSSEIR† AND CHIH-MING HO

Department of Aerospace Engineering, University of Southern California, University Park, Los Angeles

(Received 10 July 1980 and in revised form 23 April 1981)

The aerodynamic noise generated by a subsonic jet impinging on a flat plate is studied from measurements of near-field and surface-pressure fluctuations. The far-field noise measured at 90° to the jet axis is found to be generated by two different physical mechanisms. One mechanism is the impinging of the large coherent structures on the plate, and the other is associated with the initial instability of the shear layer. These two sources of noise radiate to the far field via different acoustical paths.

1. Introduction

High levels of surface-pressure fluctuations and strong feedback perturbations are generated when a jet impinges on a flat plate. In part 1 of this study (Ho & Nosseir 1981), the role of feedback in a resonant jet was investigated. Near-field pressure measurements reveal the presence of two pressure wave trains: downstream-travelling waves induced by the passage of the coherent structures, and upstream-travelling waves generated by the impingement of the coherent structures on the plate. The two wave trains were phase-locked at the nozzle exit. A new instability process is found to play a crucial role in closing the feedback loop near the nozzle lip. The thin shear layer, being forced to oscillate by the upstream-travelling waves, rolls up and forms large coherent structures at intervals phase-locked with the upstream waves. During the roll-up, many small vortices merge simultaneously into a large coherent structure over a short distance from the nozzle. This nonlinear-instability process is called the 'collective interaction'. In a resonant flow, only one time scale is allowed. This constraint is satisfied in the impinging jet owing to the collective interaction. In this paper, the noise generation of the impinging jet in both resonant and non-resonant cases is considered.

Curle (1955) described the noise generated by the flow in the presence of a solid boundary as the summation of a volume integral of quadrupoles and a surface integral of dipoles. The dipoles are produced by the fluctuating pressure exerted on the flow by the solid surface. Powell (1960) applied Curle's equation to the impinging jet. Powell's results indicated that the volume integral over the image of the jet has the same contribution to the far-field noise as does the surface integral over the plate. Marsh (1961) measured the noise generated by a jet impinging normally on a flat plate. When the plate was placed two diameters away from the nozzle the overall sound power level increased about 10 dB over that of a free jet. The excess noise decreased as the nozzle-to-plate distance increased. Preisser & Block (1976) found

† Present address: Department of Applied Science, New York University, 26–36 Stuyvesant St, New York NY 10003.

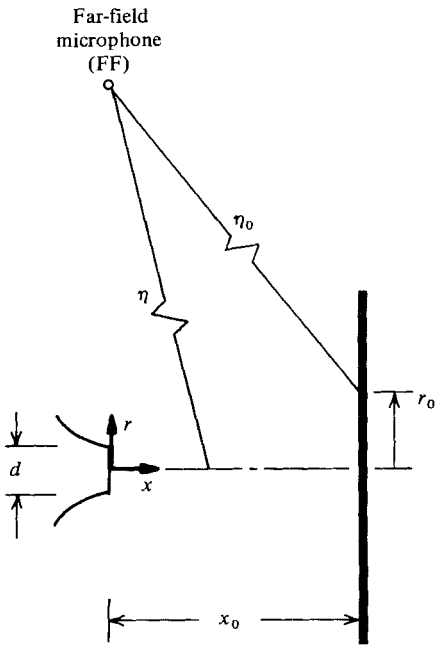

FIGURE 1.

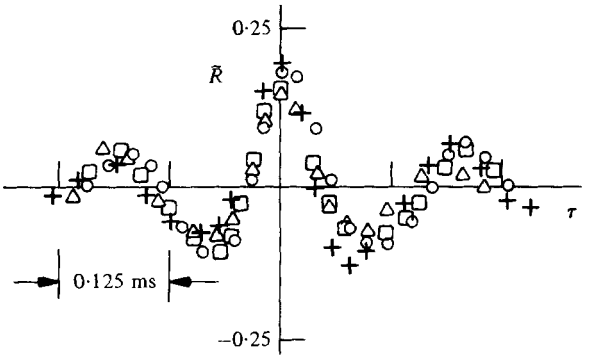

FIGURE 2.

FIGURE 1. Co-ordinate system.

FIGURE 2. Pre-whitened azimuthal correlation for a resonant jet ($M = 0{\cdot}8, x_0/d = 4, r_0/d = 1{\cdot}5$). $\Delta\phi_0$; ○, 90°; □, 135°; △, 225°; +, 270°.

that the noise generated by an impinging jet is proportional to the eighth power of the Mach number. Their measured cross-spectra indicated that most of the noise is generated in a region near the plate between one and three diameters from the stagnation point.

Identifying the main generating mechanism of jet noise has been one of the important issues pursued by many researchers. Difficulties associated with this problem are due to (i) the total noise power being generally much less than 1 % of the jet-flow power, (ii) the difficulty in using measurements of pressure fluctuations within a turbulent flow to identify the generation mechanism, (iii) diffraction and interference among the acoustic waves interacting with the shear layer (Ho & Kovasznay 1976*a*, *b*). It was therefore difficult to find a direct relationship between the far-field noise and a temporally and spatially random flow field. However, the situation became more promising after the recognition of the coherent structures as an essential feature of the free shear flow (Brown & Roshko 1971). If these structures or their interactions play an important role in the noise generation, a correlation between them and the far-field noise would likely exist owing to their organized nature and their large spatial coherence (Laufer 1974).

In the present work, an extensive study of the near-field, surface and far-field pressure fluctuations has identified the physical mechanisms of noise generation and the acoustic propagation paths. The range of the Mach number varied from 0·5 to 0·9. The nozzle-to-plate distances were limited to within the length of the potential core. The detailed description of the experimental facility and the data processing were discussed in part 1 of this study. The streamwise and the radial co-ordinates are

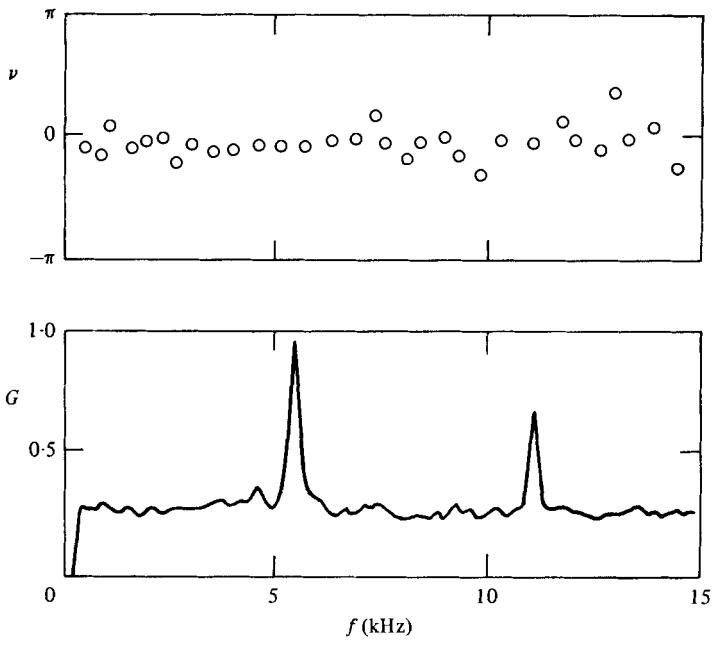

FIGURE 3. Azimuthal cross-spectrum and phase angle of surface pressure signals ($M = 0{\cdot}8$, $x_0/d = 4$, $r_0/d = 1{\cdot}5$, $\Delta\phi_0 = 90°$).

x and r respectively (figure 1). The distance between the nozzle and the plate is x_0. On the plate, the radial distance from the stagnation point is r_0 and the azimuthal angle is ϕ_0. The distance between any surface-pressure transducer and the far-field microphone is η_0, and between any near-field microphone and the far-field one is η. The far-field microphone (Bruel and Kjaer Type 4138) was placed at $\eta_n = 229$ cm away from the nozzle at 90° to the jet axis. η_n is the distance between the nozzle exit and the far-field microphone.

2. Some observed features of the flow field

2.1. *Axisymmetry of the coherent structures*

The stability analysis of Michalke (1972) indicated that both the axisymmetric and the helical modes are amplified in a jet, with their maximum amplification rates slightly different. The large coherent structures can, therefore, have either an axisymmetric or a helical shape. In a free water jet, Browand & Laufer (1975) reported that the coherent structures are axisymmetric ring vortices at small Reynolds number ($Re = UD/\nu = 5000$). A helical mode became apparent when the Reynolds number was greater than 10000. Fuchs & Michel (1977) used a set of near-field microphones placed at equal distances from the jet axis, in a plane perpendicular to the axis. From measurements of the near-field pressure induced by the coherent structures they found that the axisymmetric mode dominates over a wide range of Reynolds number ($10^4 < Re < 2 \times 10^7$), although higher modes are present. Neuwerth (1973) observed axisymmetric coherent structures in a free jet at $Re = 2{\cdot}4 \times 10^5$ ($M = 0{\cdot}5$) but a helical mode appeared at $Re = 4{\cdot}3 \times 10^5$ ($M = 0{\cdot}9$). However, when the plate was inserted, only the axisymmetric mode remained.

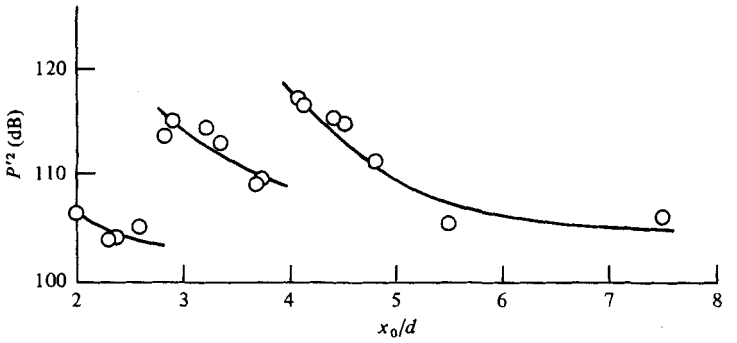

FIGURE 4. Variations of far-field noise intensity with plate locations for a resonant jet ($M = 0{\cdot}9$, $\eta_n/d = 90$).

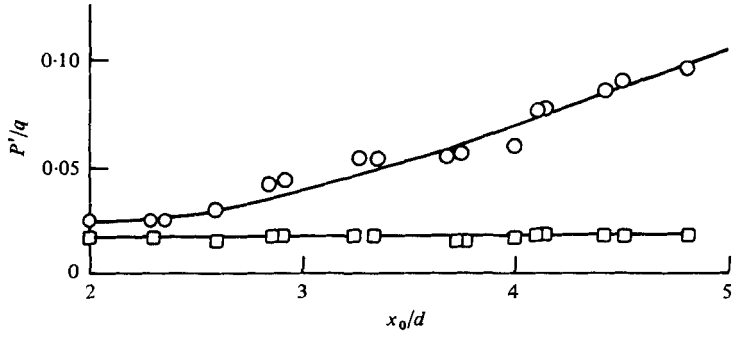

FIGURE 5. Variations of r.m.s. surface-pressure fluctuations with plate location for a resonant jet at $M = 0{\cdot}9$. ○, stagnation point($r_0/d = 0$); □, wall jet region ($r_0/d = 4$).

In the present experiment the problem of symmetry is examined in a high-Reynolds-number region by using a series of surface-pressure transducers placed at equal radial distance from the stagnation point. When the jet was in resonance ($M > 0{\cdot}7$) the cross-correlation between any two transducers at different azimuthal angles was sinusoidal with respect to the time delay τ. The correlation had a maximum at $\tau = 0$, indicating that the impinging coherent structures are dominantly axisymmetric. Such a correlation is dominated by the resonant signal. The resonant signal should be removed from the original signals in order to be able to examine the stability mode of the broad-band portions of the signals. Williams & Purdy (1970) developed a technique which is useful in a situation like this. They were able to recover the random portion of the signal by subtracting an in-phase sine wave from the original signal. This was done by analogue methods and is referred to as 'pre-whitening'. Nosseir (1979) used the same basic idea to obtain the correlation between the random portions of two signals digitally. The procedure was to replace the high resonant peak in the cross-spectrum of the original signals with the average values of the two neighbouring frequency components, and then to inverse-Fourier-transform the resulting spectrum. The correlations obtained in this way are shown in figure 2, and they still exhibit a maximum peak at $\tau = 0$, which indicates that the turbulent portion of the surface pressure fluctuations are also symmetric. This was further confirmed when the phase

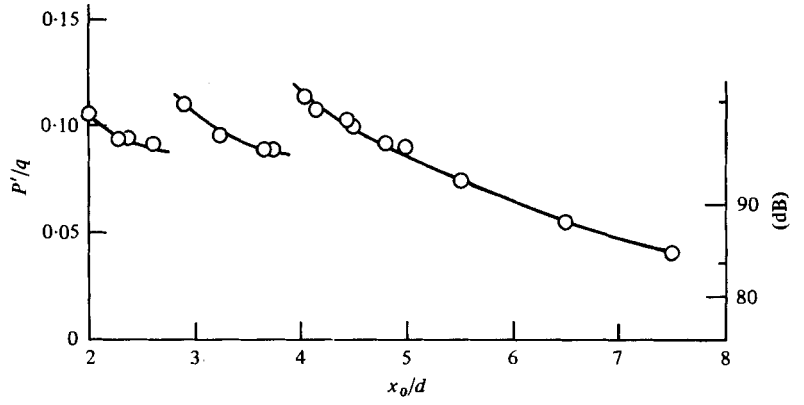

FIGURE 6. Variations of r.m.s. surface-pressure fluctuations with plate location for a resonant jet at $M = 0{\cdot}9$, vortex-impinging region ($r_0/d = 1{\cdot}5$).

difference between any two transducers was found to be approximately zero over all frequencies (figure 3). These findings guaranteed that the present far-field measurements at one azimuthal angle can be circumferentially representative.

2.2. *The relation between the far-field noise and the surface-pressure fluctuations*

2.2.1. *The far-field noise intensity.* The variation of the noise intensity with nozzle-to-plate distance for a resonant impinging jet ($M = 0{\cdot}9$) is presented in figure 4. The noise intensity has a sawtooth behaviour, with discontinuities at plate locations approximately the same as those for the frequency discontinuities in figure 14 of part 1. The sawtooth behaviour in noise frequency is also observed in other flows with self-sustained oscillations (e.g. Tam & Block 1978). It is interesting to note that the noise intensity in the impinging jet has these sawtooth variations, but they disappear for $x_0/d > 5$. This might be a result of the disintegration of the coherent structures near the end of the potential core. (However, the frequency discontinuities are observed until $x_0/d = 7{\cdot}5$.) These distinctive characteristics of the measured noise can be used to identify noise-producing regions in the flow.

2.2.2. *The surface-pressure fluctuations.* The flow visualizations in a low-Reynolds-number water jet by Nosseir (1979) and in a high-Reynolds-number resonant jet by Neuwerth (1973) showed that the large coherent structures approach the plate in a region 1·0 to 1·5 diameters from the stagnation point. Further downstream, the wall jet starts to develop. Three transducers located at $r_0/d = 0$, 1·5 and 4 are used to examine the characteristics of the pressure fluctuations in the stagnation region, the vortex-impinging region and the wall-jet region. The level of pressure fluctuations at the stagnation point (figure 5) increases steadily with increasing nozzle-to-plate distance. Strong, Siddon & Chu (1967) reported that the stagnation pressure for normal impingement reaches a maximum at $x_0/d = 7$, and then drops with further increasing x_0/d. The present measurements are limited to $x_0/d < 5$, so that the maximum is not reached. In the case of an obliquely impinging jet, the axial location, x_0/d, of maximum stagnation-pressure level is a function of incline angle (Westley, Wooley & Brossam 1972). In the wall jet, the pressure normalized to the dynamic pressure head q is constant (figure 5). The most interesting region is $1{\cdot}0 < r_0/d < 1{\cdot}5$.

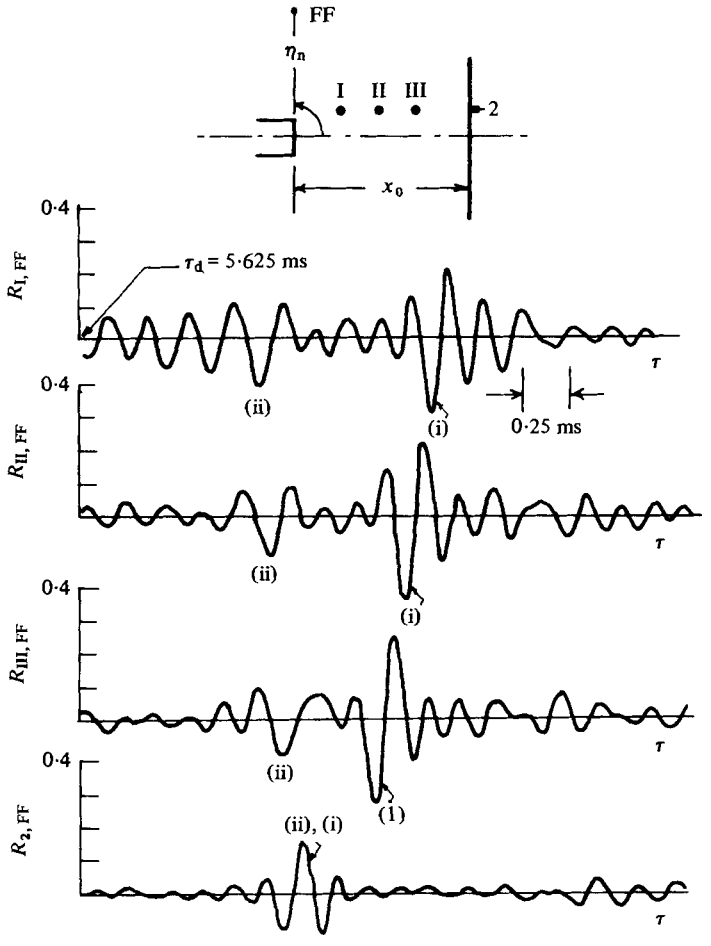

FIGURE 7. Cross-correlations with far-field microphone, point 2 is at $r_0/d = 1$ ($M = 0{\cdot}8$, $x_0/d = 5{\cdot}5$, $\eta_n/d = 90$).

mic	x/d	r/d
I	1·09	1·13
II	1·97	1·13
III	3·25	1·31

The measured pressure-fluctuation level in this region (figure 6) has discontinuities similar to, and at the same plate locations as, those observed in the noise measurements (figure 4). The sawtooth behaviour in both the noise and the surface-pressure measurements certainly implies a close relationship between the noise generation and the impinging large coherent structures. This observation is established further by the analysis of the acoustic propagation path in § 3.1.

3. The mechanisms of noise generation

3.1. *The propagation path of the noise generated by the impinging coherent structures*

Curle's (1955) analysis suggested that the noise is generated both on the solid surface and in the free jet. Although the noise from the free jet is of the quadrupole type, which

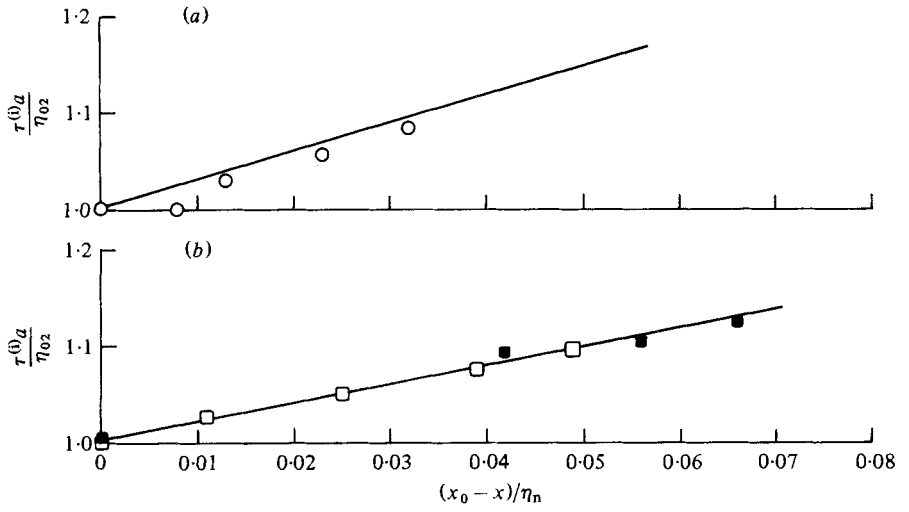

FIGURE 8. Comparison between optimum time delays of the measured correlations with the far field and equation (2), with $\eta_n/d = 90$. (*a*) $M = 0{\cdot}5$, (*b*) $M = 0{\cdot}8$. x_0/d: ○, 4; □, 5·5; ■, 7. ——, equation (2).

does not radiate as efficiently as the dipole type sound generated on the surface, the mirror-image concept used in Powell's (1960) model implied equal contributions from both types. It is almost impossible experimentally to estimate their relative contributions from far-field measurements alone, because the waves lose their original identities through interference. Therefore, far-field measurements must be complemented with near-field and surface-pressure measurements.

Cross-correlations between the far-field signal and both the near-field and the surface signals are used to determine the propagation path of the radiated pressure fluctuations. The correlation curves are shown in figure 7. The time delay in the figure is offset by 5·625 ms in order to present the main features of the correlations. A large negative peak, denoted by (i), appears in the correlations with the near-field microphones. Another smaller peak, denoted by (ii), also appears at an earlier time delay, and its significance will be discussed later. These two peaks coincide into a single positive peak in the correlation with the transducer on the plate at $r_0/d = 1{\cdot}0$.

The time delay of the maximum peak (i) in the correlation between any microphone in the near field and the far-field microphone was found to be always greater than the ratio of the distance between the two microphones divided by the ambient speed of sound. This excludes the possibility of significant direct acoustic propagation between the two. In fact, the time delay of (i) was found to satisfy the relation

$$\tau^{(i)}_{j,\mathrm{FF}} = \tau^{[1]}_{j,2} + \tau_{2,\mathrm{FF}} \quad (j = \mathrm{I}, \mathrm{II}, \mathrm{III}) \tag{1}$$

for different Mach numbers and plate locations. The first term on the right-hand side of (1), $\tau^{[1]}$, is the time delay of the maximum peak in the near-field correlations of part 1, which represents the downstream convection of the large coherent structures from point j to point 2 on the plate. The convection speed is $0{\cdot}62U$. The second term $\tau_{2,\mathrm{FF}}$ is the propagation time of the pressure waves from position 2 on the plate to the far field with the speed of sound. As mentioned before, this is the region where the large-scale structures were observed to impinge on the plate.

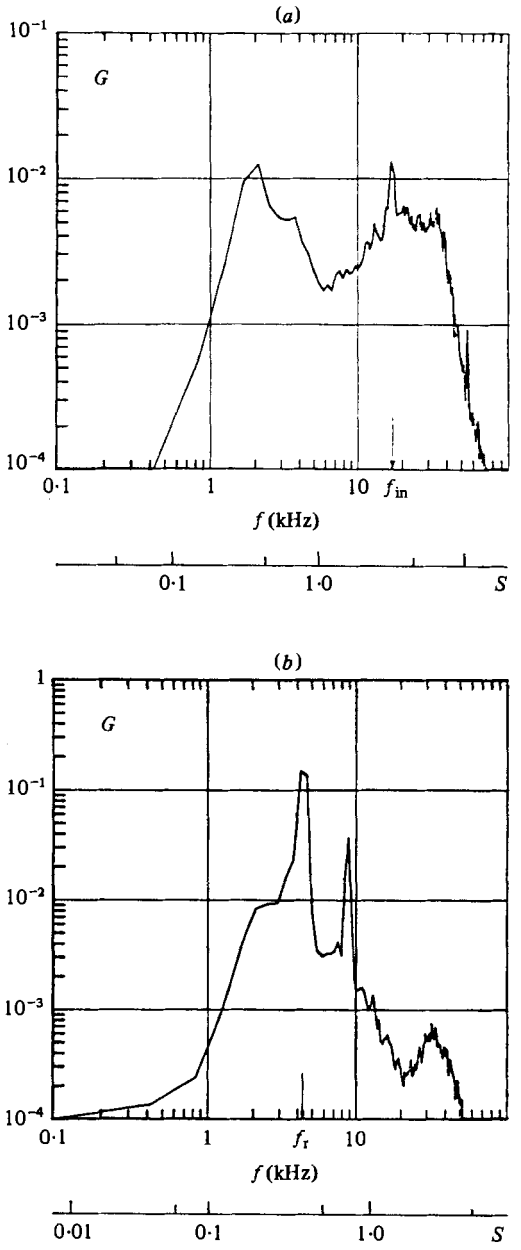

FIGURE 9. Far-field power spectra, $x_0/d = 4{\cdot}5$. (*a*) $M = 0{\cdot}4$; (*b*) $M = 0{\cdot}9$.

These experimental results indicate that most of the near-field pressure fluctuations produced by the pairing coherent structures do not dominate the noise production. The structures propagate to the surface with a speed of $0{\cdot}62U$ and then the fluctuating pressure radiates to the far field with the speed of sound. Hence, most of the noise is generated on the plate, in disagreement with the mirror-image concept (Powell 1960) which suggests that the plate contributes by only 50 % to the generated noise.

The propagation path represented by (1) holds for both resonant and non-resonant

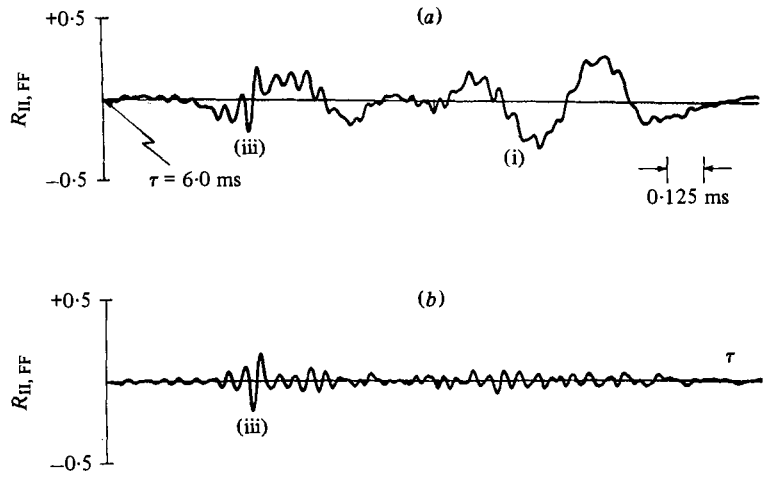

FIGURE 10. Cross-correlations between far-field and near-field signals (M = 0·4, x_0/d = 4·5, x_{II}/d = 0·92): (*a*) using raw signals; (*b*) using high-pass-filtered signals (cut-off frequency = 8 KHz).

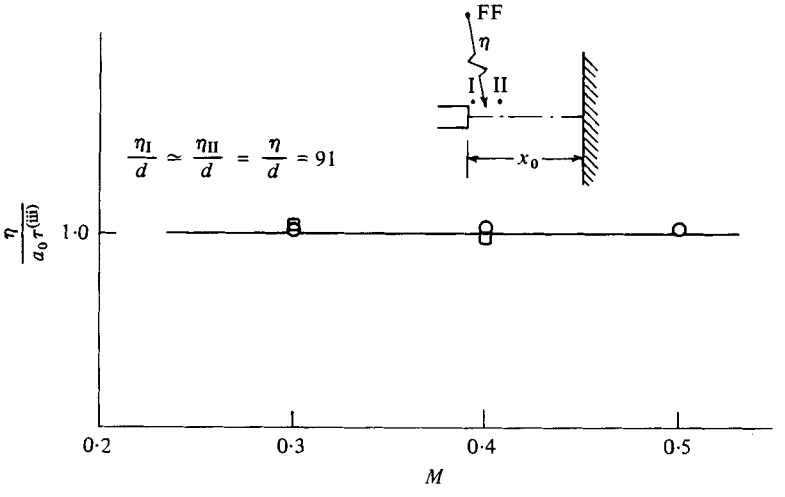

FIGURE 11. High-frequency far-field noise-radiation path, from $\tau^{(iii)}$. x_0/d = 4·5; ○, I, x/d = 0·13; □, II, x/d = 0·92.

jets. This is evident from the good agreement in figure 8 between the experimental data and (1) rewritten in the non-dimensional form

$$\frac{\tau^{(i)}a}{\eta_{02}} = 1 + \frac{x_o - x_j}{\eta_{02}} \frac{1}{MK_v} \tag{2}$$

where $K_v = C_1/U$, and C_1 is the average convection velocity of the large coherent structures. M is the Mach number. The agreement between the measured data and equation (2) for the resonant jet confirms the previous observation of the similarity in the sawtooth pressure patterns found in both the far field and in the region where the large coherent structures impinge on the plate.

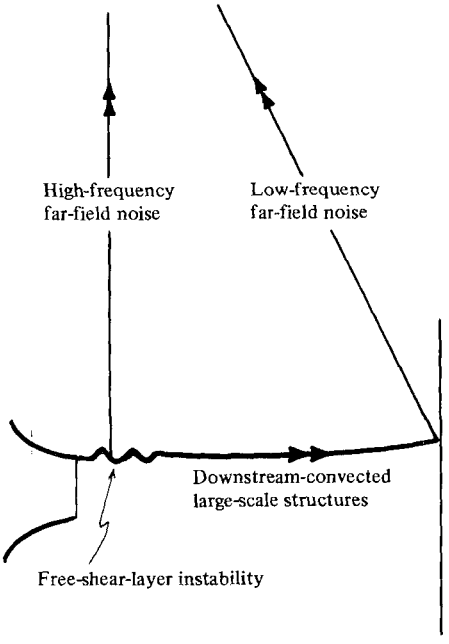

FIGURE 12. Summary of noise-generation mechanisms in an impinging jet.

In order to provide more evidence of the impinging vortices as the noise source, a very different data-processing technique, the conditional-probability-density measurement, was used to confirm the model (Nosseir & Ho 1980). First, an amplitude threshold and the positive slope were used to discriminate between events on the surface and far-field pressure fluctuations. The high-pressure fluctuations are presumably produced by the impinging vortices. The conditional-probability-density function of the time difference between the events occurring on the surface and in the far field were calculated. A pronounced peak appeared in the probability-density function and is equal to the acoustic-wave-propagation time from the plate to the far field. Two minor peaks on both sides of the main peak represent the frequency of events. The periods of these two minor peaks are in the range associated with the passage frequency of the large coherent structures on the plate. Hence the conditional-probability function supports the conclusions arrived from the correlation measurement.

The explanation of the characteristics of the correlations in figure 7 is, in itself, compatible with the above findings. Lau, Fisher & Fuchs (1972) showed that a negative pressure disturbance is recorded whenever an eddy passes a near-field microphone. When this eddy impinges on the plate, a positive pressure disturbance is recorded by the surface-pressure transducer. (Ho & Kovasznay (unpublished) have measured positive-pressure disturbances associated with the impingement of isolated ring vortices on a flat plate.) This disturbance propagates to the far field, and accordingly a positive peak appears in the correlation with the surface pressure (e.g. $R_{2,\,\mathrm{FF}}(\tau)$). On the other hand, the same positive disturbance at the far field would have been measured earlier as a negative one in the near field, resulting in a negative peak (e.g. $R_{\mathrm{I},\,\mathrm{FF}}(\tau)$). Furthermore, as the large coherent structures impinge on the plate, acoustic waves are not only radiated to the far field, but also back to the near-field microphone

(see part 1). This results in the appearance of peak (ii). The difference in the time delays of (i) and (ii) decreases as the signal from the far field is correlated with locations closer to the plate (eventually both peaks coincide in the correlation with the transducer on the plate). Therefore, peak (ii) does not correspond to direct acoustic radiation between the near field and the far field.

3.2. *Spectra of the far-field noise*

When the spectra of the far-field signals were examined, they revealed that the impingement of the large coherent structures on the plate is not the only mechanism for the generation of noise. The spectra in figures 9(*a*, *b*) display two characteristic peaks. Figure 9(*a*) shows a spectral peak at a Strouhal number of 0·33, which corresponds to the noise generated by the impinging coherent structures. Another peak appears at a higher-frequency band centred on the shear-layer instability frequency which was measured near the nozzle lip in part 1. The two peaks have the same level; however, since the energy is an integration over frequency, most of the noise energy is associated with the high-frequency instability waves of the thin shear layer for this low-Mach-number case ($M = 0{\cdot}4$). A similar distribution of energy (figure 9*b*) is observed for a resonant jet at $M = 0{\cdot}9$, except that in this case the large coherent structures prevail and a considerable amount of energy is concentrated at the resonant frequency and its first harmonic. The mechanism associated with such efficient high-frequency noise radiation might be an unsteady loading on the nozzle lip induced by the instability vortices, which would produce a dipole-type sound. Another possibility is the flapping of the thin shear layer (part 1), which would force the mean flow to undergo acceleration and deceleration. This would lead to oscillations of the mass-flow rate, producing a monopole sound field. However, both hypotheses are extremely difficult to prove experimentally.

3.3. *The radiation path of the noise generated by the instability waves*

The high-frequency instability waves, or small vortices, evolve downstream into large coherent structures. This takes place over a short distance from the nozzle by the collective-interaction process (part 1). Therefore, the high-frequency noise associated with the instability waves cannot follow the same path discussed earlier because the waves lose their identity long before they reach the plate.

Cross-correlation between the far-field microphone and a near-field microphone placed near the nozzle exit is shown in figure 10(*a*). A broad negative peak (i) is associated with the noise generated by the impinging coherent structures. Another peak, denoted by (iii), emerges at an earlier time delay. In order to ensure that this peak corresponds to the radiated high-frequency noise, the pressure signals were filtered using a high-pass filter. The cut-off frequency of the filter was chosen to be the 8 kHz frequency of the valley between the two spectral peaks in figure 9(*a*). The correlation of the filtered signals is shown in figure 10(*b*). Although peak (i) disappeared, peak (iii) survived. The noise radiation path is determined from the time delay of peak (iii). The time delay, in the nondimensional form $\eta/a\tau^{(iii)}$, is plotted in figure 11. The data collapse onto a straight line at $\eta/a\tau^{(iii)} = 1{\cdot}0$, indicating direct high-frequency acoustic radiation to the far field.

Correlations made for resonant cases have similar features. However, the correlation coefficients of peak (iii) were low, because of the low intensity of the high-frequency

noise relative to the low-frequency noise (figure 12*b*). Also, peak (iii) did not appear in the correlations with near-field microphones placed farther downstream, as expected, because of the collective interaction.

4. Conclusion

Both the generating mechanisms and the propagation paths of the far-field noise in a subsonic impinging jet were clarified through the present study (figure 12). The large coherent structures and the initial instability waves are responsible for the noise measured at 90° to the jet axis. Most of the noise generated by the coherent structures is caused by their impingement on the plate. The noise produced by these structures in the free-jet region is minimal in comparison. The noise associated with the instability waves of the shear layer radiates directly from near the nozzle exit. The collective interaction (part 1) confines the evolution of high-frequency instability waves into large coherent structures to a short distance, such that the two noise-generating mechanisms are spatially separated.

The authors would like to thank Dr J. Laufer for his continuous encouragement and helpful discussions during the course of this study. This work was sponsored by AFOSR under grant 77-3312 and contract F49620-78-C-0060.

REFERENCES

Brown, G. & Roshko, A. 1971 The effect of density differences on the turbulent mixing layer. *AGARD Conf. Proc.*, no. 93, paper 23.

Browand, F. K. & Laufer, J. 1975 The role of large scale structures in the initial development of circular jets. In *Proc. 4th Biennial Symp. on Turbulence in Liquids, University of Missouri–Rolla* (ed. J. L. Zakin & G. K. Patterson), pp. 333–344. Science Press.

Curle, N. 1955 The influence of solid boundaries upon aerodynamic sound. *Proc. R. Soc. Lond.* A **231**, 505–514.

Fuchs, H. V. & Michel, U. 1977 Experimental evidence of turbulent source coherence affecting jet noise. *A.I.A.A. Paper* no. 77–1348.

Ho, C.-M. & Kovasznay, L. S. G. 1976*a* Acoustical shadowgraph. *Phys. Fluids* **19**, 1118–1123.

Ho, C.-M. & Kovasznay, L. S. G. 1976*b* Propagation of coherent acoustic wave through a turbulent shear flow. *J. Acoust. Soc. Am.* **60**, 40–45.

Ho, C.-M. & Nosseir, N. S. 1981 Dynamics of an impinging jet. Part 1. The feedback phenomenon. *J. Fluid Mech.* **105**, 119–142.

Lau, J. C., Fisher, M. J. & Fuchs, H. V. 1972 The intrinsic structure of turbulent jets. *J. Sound Vib.* **22**, 379–406.

Laufer, J. 1974 On the mechanism of noise generation by turbulence. In *Omaggio a Carlo Ferrari*, pp. 449–464. Libreria Editrice Universitaria Levrotto & Bella.

Marsh, A. H. 1961 Noise measurements around a subsonic air jet impinging on a plane, rigid surface. *J. Acoust. Soc. Am.* **33**, 1065–1066.

Michalke, A. 1972 Instabilität eines Kompressiblen runden freistrahls unter berücksichtigung des einflusses der strahlgrenzschicktdicke. *Z. Flugwiss.* **19**, 319–328.

Neuwerth, G. 1973 Dr-Ing. thesis. Technische Hochschule, Aachen, West Germany.

Nosseir, N. S. 1979 On the feedback phenomenon and noise generation of an impinging jet. Ph.D. thesis, University of Southern California.

Nosseir, N. S. & Ho, C. M. 1980 Pressure fields generated by instability waves and coherent structures in an impinging jet. *A.I.A.A. Paper* no. 80–0980.

Powell, A. 1960 Aerodynamic noise and the plane boundary. *J. Acoust. Soc. Am.* **32**, 982–990.

Preisser, J. S. & Block, P. J. W. 1976 An experimental study of the aeroacoustics of a subsonic jet impinging normal to a large rigid surface. *A.I.A.A. Paper* no. 76–520.

STRONG, D. R., SIDDON, T. E. & CHU, W. T. 1967 Pressure fluctuations on a flat plate with oblique jet impingement. *N.A.S.A.* CR-839.

TAM, C. & BLOCK, P. J. W. 1978 On the tones and pressure oscillations induced by flow over rectangular cavities. *J. Fluid Mech.* **89**, 373–399.

WILLIAMS, K. C. & PURDY, K. R. 1970 A prewhitening technique for recording acoustic turbulent flow data. *Rev. Sci. Instrum.* **41**, 1897–1899.

WESTLEY, R., WOOLLEY, J. H. & BROSSAM, P. 1972 Surface pressure fluctuations from jet impingement on an inclined plate. *Symp. on Acoustic Fatigue, Toulouse. AGARD Conf. Reprint* no. 113.